ELSEVIER

Magnetic Resonance Materials in Physics, Biology and Medicine 15 (2002) 52–57

MAGMA
Magnetic Resonance Materials in Physics, Biology and Medicine

www.elsevier.com/locate/magma

MR-velocity mapping in vascular stents to assess peak systolic velocity. In vitro comparison of various stent designs made of Stainless Steel and Nitinol

Jacqueline van Holten [a,*], Patrik Kunz [b], Paul G.H. Mulder [c], Peter M.T. Pattynama [a], Hildo J. Lamb [b], Lukas C. van Dijk [a]

[a] *Department of Radiology, Erasmus MC, University Medical Center Rotterdam, Dr Molewaterplein 40, 3015GD Rotterdam, The Netherlands*
[b] *Department of Radiology, Leiden University Medical Center, Leiden, The Netherlands*
[c] *Department of Epidemiology and Biostatistics, Erasmus University Medical Center Rotterdam, Rotterdam, The Netherlands*

Abstract

Introduction: Peak systolic velocity (PSV) measurements of blood flow inside vascular stents allow reliable detection of in-stent re-stenosis. The purpose of this in vitro study was to evaluate the feasibility of obtaining PSV measurements inside vascular stents made of Stainless Steel and Nitinol, using a velocity encoded MR technique. *Materials/methods:* In a flow phantom, stents of Stainless Steel and Nitinol were studied. The phantom was integrated into a closed-tubing circuit driven by a MR dedicated pulsatile flow pump. MR imaging was performed on a 1.5 T system. The PSV in the tube without stent was used as the gold standard to determine the accuracy and the variability (paired t-test and Pittman's test) of the PSV measurements inside the stents. *Results:* PSV values inside the stents showed percentual difference in mean of -15 to 21% ($P < 0.05$) at a pump setting of 10 and 20 ml/s. *Conclusion:* PSV measurements can be accurately obtained inside stents made of Stainless Steel and Nitinol. MR-velocity measurements may be used in patients to non-invasively evaluate stent patency and in-stent re-stenosis.

Keywords: MR angiography; Stents; Vascular; Artifacts

1. Introduction

The use of MRA for non-invasive vascular imaging in routine clinical practice is steadily increasing [1,2]. However, the utility of MRA may be hampered after treatment with vascular stents. The metal stents generally cause two types of artifacts in MR imaging that render the morphological evaluation of any in-stent re-stenoses unreliable [3,4]; magnetic susceptibility artifacts and the less well known radio frequency (RF) artifacts. Imaging of the stented artery during follow-up is important because in-stent re-stenosis after stent placement frequently, e.g. occurs in 5–15% in iliac arteries [5–7] and 11–78% in the coronary arteries [8–10].

The most commonly used vascular stents in the non-coronary arteries are made of Stainless Steel, Elgiloy or Nitinol. For coronary artery stenting Stainless Steel-316 is almost ubiquitously used. Of these metal alloys, Stainless Steel and Elgiloy cause the worst magnetic susceptibility artifacts in MR imaging, whereas Nitinol causes relatively mild susceptibility artifacts [3,11,12]. RF artifacts are associated with a decrease of signal inside the stent lumen, which may be present in all metal stents including in the ones made of Nitinol.

In general terms, in-stent re-stenosis can be detected, not only by imaging the morphological luminal narrowing, but alternatively, also by analyzing the flow profile inside the stent, in particular, by measuring the peak systolic velocity (PSV). This feature is well known and used in clinical practice in ultrasound Doppler-imaging of arteries, by measuring the PSV in a stenosis and comparing it with the PSV upstream (a PSV-ratio of > 2 is generally held to indicate a diameter stenosis of $>$ 50%) (Coffi, 2001 #163) (Ranke, 1992 #164).

* Corresponding author. Tel.: +31-10-4639222; fax: +31-10-4634033
E-mail address: vanholten@rond.azr.nl (J. van Holten).

1352-8661/02/$ - see front matter
PII: S1352-8661(02)00124-2

Quantitative MR flow mapping also provides accurate measurements of flow velocity (and flow volume) inside the vessel [14,15], which is already in routine clinical use to quantify stenosis in aortic coarctation [16]. Therefore, it is proposed here, quantitative MR imaging may be used for detection and quantification of haemodynamic significant in-stent stenosis.

The purpose of the present study was to evaluate the feasibility of PSV measurements inside different vascular stents made of Stainless Steel and Nitinol, using a velocity encoded MR technique.

2. Methods

2.1. Flow phantom design

The phantom consisted of four parallel plastic tubes of equal size (each with a of length 15 cm and inside diameter of 10 mm) that were connected in a serial fashion, in which all stents were implanted, (Fig. 1). This phantom was integrated into a closed-tubing circuit driven by a MR compatible computer-controlled pulsatile flow pump (UHDC flow system MR version, Quest Imaging Incorporated, London, Ontario, Canada). Two custom made stents ($\varnothing = 10$ mm, length $= 40$ mm) made of Stainless Steel and Nitinol, respectively, and four commercial stents ($\varnothing = 10$ mm) were studied (Table 1). The custom made stents were wire-woven and of identical design and with a wire diameter of 0.1 mm. A bi-phasic flow pattern with a frequency of 60 per min was applied and the pump was adjusted to deliver flow rates of 10 and 20 ml/s. An ECG signal was synchronized to the flow cycle and used for prospective triggering of the MR-scanner during image acquisition.

We used MR BLOOD-MIMICKING® fluid in the flow phantom, which had magnetic relaxation parameters and shear viscosity similar to human blood (Shelley Medical Imaging Technologies, Acra Techn, Quebec, Canada). The phantom was placed in a water-filled plastic container.

Table 1
Metallic vascular devices

Material	Type	Manufacturer
Stainless Steel-316	Custom made (l = 40 mm, $\varnothing = 10$ mm)	–
	Corinthian® (l = 25 mm, $\varnothing = 10$ mm)	Cordis (Miami, FL)
	Megalink® (l = 30 mm, $\varnothing = 10$ mm)	Guidant (Temecula, CA)
Nitinol	Custom made (l = 40 mm, $\varnothing = 10$ mm)	–
	ZA stent® (l = 77 mm, $\varnothing = 10$ mm)	Cook (Bjaeverskov, Denmark)
	S.M.A.R.T.stent® (l = 36 mm, $\varnothing = 10$ mm)	Cordis

Metallic vascular devices, which were evaluated.

2.2. MRI technique

MR imaging was performed using a 1.5 T system (Gyroscan, ACS-NT15; Philips Medical Systems, Best, The Netherlands) equipped with a 5-element synergy surface coil for signal reception. For imaging, the plastic tubes containing the stents were positioned in the center of the bore parallel to the main magnetic field (B_0). Scout images were obtained with a gradient-echo sequence to plan the flow velocity encoded MR sequences. Phase contrast MR-velocity mapping was performed in a plane transverse to the long axis of the stents and by using a two-dimensional flow-sensitive gradient-echo sequence. Velocity encoding was perpendicular to the imaging plane and thus, parallel to the

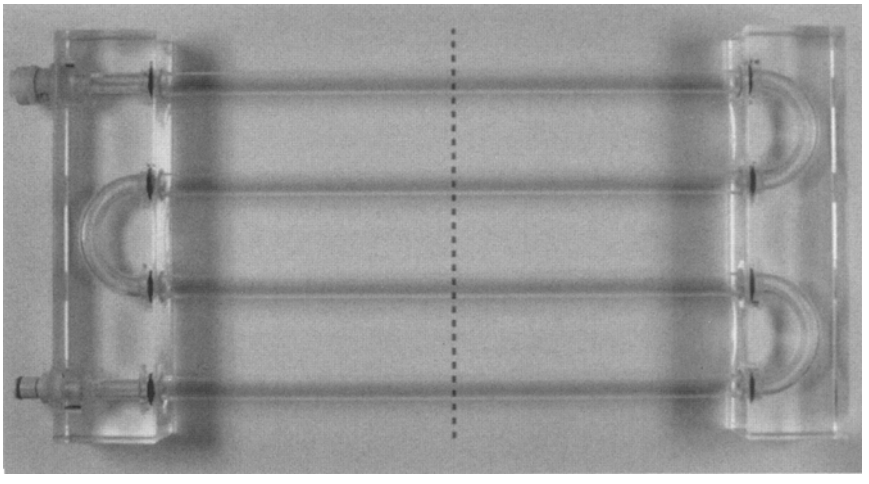

Fig. 1. The phantom consisted of four tubes with a length of 15 cm and a diameter of 10 mm, connected in series. This phantom was integrated into a closed circuit. The stents were placed in the middle of the tubes. The dotted line indicates the measurement site of the velocity mapping.

long axis of the stents. Velocity sensitivity was set at 30 or 60 cm/s depending on the flow pump settings to avoid signal aliasing. Other imaging parameters were: TR = 1000 ms, TE = 4.2 ms, flip angle = 25°, field of view = 210 mm (RFOV 50%), matrix = 256 × 102, section thickness = 6 mm and temporal resolution = 95 sample points per heart beat at a heart rate of 60 beats/min. Total scan time was 3:20 min per experiment.

2.3. MR imaging analysis

The MR images were transferred to an Ultra-1-Sparc workstation (SUN Microsystems, Mountain View, CA). Flow velocity encoded MR imaging data were analyzed by using the MR analytical software system (version 3.0) with dedicated software package, FLOW®, developed in our department (Leiden University Medical Center).

The PSV was determined by using central lumen curves and analyzing the maximum velocity in these curves. Central lumen curves were obtained by using 9 pixels taken from the center of the lumen (pixel size 0.8×1.0 mm^2, the same as the original scan data). The velocity curves were then calculated by automatic measurement within these 9 pixels. PSV was calculated by time-averaging the nine measurement values around the maximum velocity (Fig. 2). We also measured the surface of the visible lumen inside the stent and inside the tube without stent.

2.4. Data analysis

Data analysis was done by an independent biostatistician (PGHM). The PSV in the tube without stent was used as the gold standard to determine the accuracy and reliability of the PSV measurements inside the stents.

We analyzed the PSV inside the stents and the tube without stent at two different pump settings, 10 and 20 ml/s. First, it was of interest whether the PSV measured in a stent was significantly different from that in the tube without stent. This was done by using a paired Student t-test at $P = 0.05$. This test indicated whether or not the MR-based PSV measured in stents were accurate. Next, we tested whether the S.D. of the nine measured values around PSV were different between the stented and the non-stented segment. This was done by using the Pitman's test at $P = 0.05$ [17]. A Pitman's test of $P < 0.05$ indicated a significantly greater variability (more noisy) measurement compared to the tube without stent. (Pitman's test was used to test the null hypothesis that two variances of paired measurements are the same. The null hypothesis is identical to a zero Pearson correlation between the sum and the difference of two paired measurements.)

In a control experiment, we analyzed whether the underlying assumption used in our study was indeed correct, i.e., that the actual PSV in the empty part of the tubing was the same as that in the parts of the tubing that contained the metal stents. This was done by using Doppler ultrasound (Aloka, Tokyo, Japan and a 7.5-MHz linear-array transducer) to validate the phantom and by using ULTRASOUND BLOOD MIMICKING® fluid (Shelley Medical Imaging Technologies) at the same pump settings used in the MR experiment (10 and 20 ml/s).

We quantified the influence of magnetic susceptibility artifacts on the evaluation of the stent lumen area. The visible lumen area inside the stent was measured. The (virtual) lumen reduction was calculated by dividing the virtual lumen area inside the stent by the true lumen area in the tube without stent.

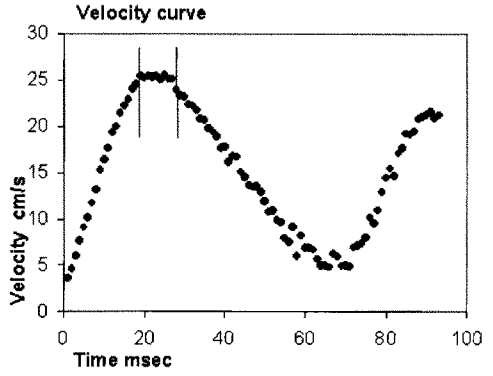

Fig. 2. Flow curve of the tube without stent, with the pump set at 20 ml/s flow rate. PSV was determined by time-averaging nine measured values (between the gray lines) around the maximum velocity in the flow curves of each stent.

3. Results

The control experiment using Doppler ultrasound confirmed the validity of our assumption that the PSV

Table 2
The results of the Doppler ultrasound experiment to validate the phantom

Bi-phasic flow pattern	Pump setting	
Doppler ultrasound, PSV	10 ml/s	20 ml/s
Stent without stent	0.25 m/s	0.43 m/s
Stainless Steel, Corinthian®	0.26 m/s	0.47 m/s
Stainless Steel, Megalink®	0.25 m/s	0.42 m/s
Stainless Steel, custom made	0.22 m/s	0.46 m/s
Nitinol, S.M.A.R.T.stent®	0.26 m/s	0.46 m/s
Nitinol, ZA stent®	0.23 m/s	0.41 m/s
Nitinol, custom made	0.23 m/s	0.42 m/s

The PSV in the tube without stent was not significantly different from that in the stent-containing tube segments, which indicates that the PSV was constant throughout the entire flow phantom.

in the tube without stent is the same as the PSV in the tubes containing the stents (Table 2).

Table 3 shows PSV measurements at a pump setting of 10 ml/s. The PSV inside the stents was statistically significant different from that in the tube without stent. The extent of this difference, however, was acceptable considering the proposed use of determining PSV-ratios >2 and ranged from -15 to 5.6%. The PSV measurements of the Corinthian® and the Megalink® Stainless Steel stents showed more variability and therefore had a statistically significant difference of S.D. of the PSV compared to the tube without stent. The other stents showed no statistically significant difference of the S.D. compared to the S.D. of the tube without stent.

The results of the PSV at a pump setting of 20 ml/s are presented in Table 3. The PSV showed a statistically difference ranging from -9 to 21% in the various stents as compared to the tube without stent. The Stainless Steel Megalink® stent, the custom made Stainless Steel stent and the custom made Nitinol stent showed no statistically significant difference in S.D. compared to the tube without stent. In the other three stents the S.D. of the peak velocity measurements were significantly higher.

Fig. 3 illustrates the imaging MR artifacts of each stent. The stents made of Stainless Steel had the most extensive magnetic susceptibility artifacts, which created a reduction of the surface area of the visible lumen inside the Stainless Steel stents (Table 4). Magnetic susceptibility artifacts were more pronounced at the edges of the different stents. The RF artifact was most obvious inside the stents made of Nitinol. The Nitinol S.M.A.R.T. stent® and the Stainless Steel Corinthian® stent were associated with the most pronounced signal loss inside the stent lumen.

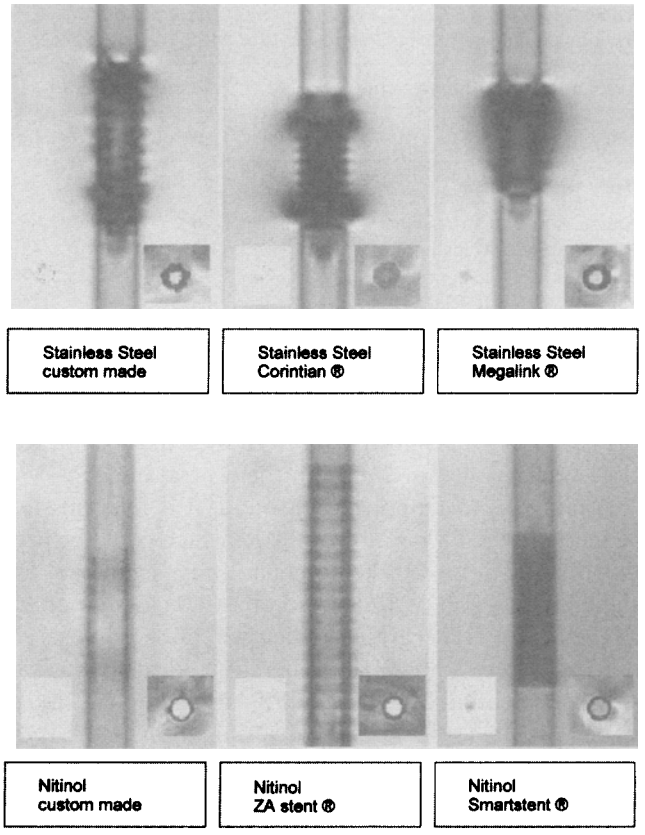

Fig. 3. Coronal MR scout images and axial MR images of the used vascular stents showing the different artifacts of each stent. (See text for detailed discussion.)

4. Discussion

Our experiments show that assessment of PSV measurements inside vascular stents by velocity encoded MRI is feasible. Despite the fact that signal void is often

Table 3
The results of the PSV measurements at a pump setting of 10 and 20 ml/s

PSV	Pump setting 10 ml/s				Pump setting 20 ml/s			
	PSV cm/s	P paired-t	S.D.	Pitman's test P	PSV cm/s	P paired-t	S.D.	Pitman's test P
Tube without stent	25.84		0.22		46.02		0.45	
Stainless Steel, Corinthian	21.84	<0.05	4.9	<0.05	41.95	<0.05	1.95	<0.05
% difference versus without stent	−15%				−9%			
Stainless Steel, Megalink	27.3	<0.05	0.62	<0.05	55.48	<0.05	0.36	0.57
% difference versus without stent	5.7%				21%			
Stainless Steel, custom made stent	26.11	<0.05	0.18	0.51	49.04	<0.05	0.33	0.38
% difference versus without stent	1.0%				7%			
Nitinol, S.M.A.R.T.stent	26.27	<0.05	0.45	0.05	52.66	<0.05	1.23	<0.05
% difference versus without stent	1.7%				14%			
Nitinol, ZA stent	24.21	<0.05	0.14	0.23	51.13	<0.05	0.96	<0.05
% difference versus without stent	−6.3%				11%			
Nitinol, custom made stent	24.08	<0.05	0.16	0.29	44.56	<0.05	0.56	0.34
% difference versus without stent	−6.8%				−3%			

Table 4
The lumen reduction compared to the tube without stent for each stent in the mean velocity measurements

Lumen reduction pump setting	10 ml/s		20 ml/s	
	Area (mm^2)	Lumen reduction (%)	Area (mm^2)	Lumen reduction (%)
Tube without stent	76	–	88	–
Stainless Steel, Corinthian®	26	66	20	78
Stainless Steel, Megalink®	44	42	36	59
Stainless Steel, custom made	33	57	26	71
Nitinol, S.M.A.R.T.stent®	65	15	65	27
Nitinol, ZA stent®	57	26	65	27
Nitinol, custom made	69	8	76	14

present, this seems not to interfere with the accuracy of flow velocity measurements in the central lumen.

Analogous to Doppler ultrasound, it is thus possible to measure the PSV-ratio with MR, which could be used for quantification of hemodynamically significant in-stent stenosis [13]. A PSV-ratio of >2.0 (100% increase of velocity) is generally indicative of a stenosis of approximately $\geqslant 50\%$ [18]. Therefore, despite the observed percentual difference in PSV measurements in the various stents (-15 to 21%), determination of the PSV-ratio might be used for evaluation of in-stent stenosis. Only for the Stainless Steel Corinthian® stent the MR-velocity measurement appears to be unreliable (Pitman test $P \ll 0.05$).

Quantitative MR flow mapping has proven to be an accurate and reliable technique for estimating blood flow velocity as well as volume flow [14,19,20]. To our knowledge only two previous studies have used quantitative MR flow measurements before and after stent placement [21,22]. Velocity measurements were done proximally and distally to the stent, however, which implies that the site of maximum vessel stenosis was likely missed. The authors did not mention if velocity mapping inside the stent was possible.

Whereas PSV measurements only rely on imaging the central part of the vessel lumen, measurements of volume flow involve quantification of the entire surface area of the vessel. As expected the stents showed magnetic susceptibility artifacts. The stents made of Stainless Steel caused more extensive magnetic susceptibility artifacts than the stents made of Nitinol [3,4,12,23]. These artifacts preclude the calculation of accurate volume flow inside stents because they cause lumen reduction on the image (Table 4).

Evaluation of in-stent morphology using MRA with or without contrast-enhancement is limited because of image artifacts caused by metal alloys. The two main types of artifacts that are associated with metallic vascular implants in MR are the magnetic susceptibility artifacts and RF artifacts [24,25]. The magnetic susceptibility artifacts arise from metal induced local field inhomogenities and are located around the stent material. The RF artifact is caused by electromotive forces in stents, which are induced in loops of the vascular implant by the time-varying magnetic field component of the RF waves. These forces cause eddy currents, which cause attenuated signal inside the stent [25]. Especially stents made of ferromagnetic material such as Stainless Steel show extensive susceptibility artifacts. With the introduction of stents made of the more MR-compatible paramagnetic material Nitinol, susceptibility artifacts became less of a problem. However RF artifacts remain an issue, as was also shown in the current study.

Our results show that stents made of Nitinol as well as Stainless Steel are associated with RF artifacts. The extent of attenuation (caused by the RF artifact) inside the various stents varied with stent designs, even in stents made of the same material (Fig. 3). Thus RF artifacts in vascular stents depend on both stent design and stent material as a conclusion also put forward by others [24]. It is uncertain, whether our results can be applied to stents of other designs or dimensions.

4.1. Practical application

Central lumen PSV measurements with velocity encoded Phase Contrast-MR may become useful in the clinical setting to evaluate stent patency and quantify in-stent stenoses in Nitinol and even in some Stainless Steel vascular stents.

References

[1] Volk M, Strotzer M, Lenhart M, Manke C, Nitz WR, Seitz J, et al. Time-resolved contrast-enhanced MR angiography of renal artery stenosis: diagnostic accuracy and interobserver variability. Am J Roentgenol 2000;174(6):1583–8.
[2] Mitsuzaki K, Yamashita Y, Sakaguchi T, Ogata I, Takahashi M, Hiai Y. Abdomen, pelvis, and extremities: diagnostic accuracy of dynamic contrast-enhanced turbo MR angiography compared with conventional angiography-initial experience. Radiology 2000;216(3):909–15.

[3] Hilfiker PR, Quick HH, Debatin JF. Plain and covered stent-grafts: in vitro evaluation of characteristics at three-dimensional MR angiography. Radiology 1999;211(3):693–7 (see comments).
[4] Meyer JM, Buecker A, Schuermann K, Ruebben A, Guenther RW. MR evaluation of stent patency: in vitro test of 22 metallic stents and the possibility of determining their patency by MR angiography. Invest Radiol 2000;35(12):739–46.
[5] Lee ES, Steenson CC, Trimble KE, Caldwell MP, Kuskowski MA, Santilli SM. Comparing patency rates between external iliac and common iliac artery stents. J Vasc Surg 2000;31(5):889–94.
[6] van Walraven LA, Andhyiswara T, van der Linden TN, Yo TI. The use of vascular stents in the treatment of iliac artery occlusion. Int J Angiol 2000;9(4):232–5.
[7] Cheng SW, Ting AC, Lau H, Wong J. Immediate stenting of iliofemoral occlusive lesions: a surgeon's early experiences. J Endovasc Surg 1999;6(3):256–63.
[8] Gyongyosi M, Yang P, Khorsand A, Glogar D. Longitudinal straightening effect of stents is an additional predictor for major adverse cardiac events. Austrian Wiktor Stent Study Group and European Paragon Stent Investigators. J Am Coll Cardiol 2000;35(6):1580–9.
[9] Hopp HW, Baer FM, Ozbek C, Kuck KH, Scheller B. A synergistic approach to optimal stenting: directional coronary atherectomy prior to coronary artery stent implantation—the AtheroLink Registry. AtheroLink Study Group. J Am Coll Cardiol 2000;36(6):1853–9.
[10] Di Sciascio G, Patti G, Nasso G, Manzoli A, D'Ambrosio A, Abbate A. Early and long-term results of stenting of diffuse coronary artery disease. Am J Cardiol 2000;86(11):1166–70.
[11] van Dijk LC, van Holten J, van Dijk BP, Matheijssen NA, Pattynama PM. A precious metal alloy for construction of MR imaging-compatible. Radiology. 2001 April;219(1):284–7.
[12] Hilfiker PR, Quick HH, Pfammatter T, Schmidt M, Debatin JF. Three-dimensional MR angiography of a nitinol-based abdominal aortic stent graft: assessment of heating and imaging characteristics. Eur Radiol 1999;9(9):1775–80.
[13] Hoppe M, Heverhagen JT, Froelich JJ, Kunisch-Hoppe M, Klose KJ, Wagner HJ. Correlation of flow velocity measurements by magnetic resonance phase contrast imaging and intravascular Doppler ultrasound. Invest Radiol 1998;33(8):427–32.
[14] Walker MF, Souza SP, Dumoulin CL. Quantitative flow measurement in phase contrast MR angiography. J Comput Assist Tomogr 1988;12(2):304–13.
[15] Frayne R, Steinman DA, Ethier CR, Rutt BK. Accuracy of MR phase contrast velocity measurements for unsteady flow. J Magn Reson Imaging 1995;5(4):428–31.
[16] Engvall J, Sjoqvist L, Nylander E, Thuomas KA, Wranne B. Biplane transoesophageal echocardiography, transthoracic Doppler, and magnetic resonance imaging in the assessment of coarctation of the aorta. Eur Heart J 1995;16(10):1399–409.
[17] Pitman E. A note on normal correlation. Biometrika 1939;31:9–12.
[18] Sensier YJ, Thrush AJ, Loftus I, Evans DH, London NJ. A comparison of colour duplex ultrasonography, papaverine testing and common femoral Doppler waveform analysis for assessment of the aortoiliac arteries. Eur J Vasc Endovasc Surg 2000;20(1):29–35.
[19] Debatin JF, Leung DA, Wildermuth S, Botnar R, Felblinger J, McKinnon GC. Flow quantitation with echo-planar phase-contrast velocity mapping: in vitro and in vivo evaluation. J Magn Reson Imaging 1995;5(6):656–62.
[20] Kroft LJ, Simons P, van Laar JM, de Roos A. Patients with pulmonary fibrosis: cardiac function assessed with MR imaging. Radiology 2000;216(2):464–71.
[21] Engellau L, Olsrud J, Brockstedt S, Albrechtsson U, Norgren L, Stahlberg F, et al. MR evaluation ex vivo and in vivo of a covered stent-graft for abdominal aortic aneurysms: ferromagnetism, heating, artifacts, and velocity mapping. J Magn Resonance 2000;12(1):112–21 (In Process Citation).
[22] Nagel E, Hug J, Bunger S, Bornstedt A, Schnackenburg B, Wellnhofer E. Coronary flow measurements for evaluation of patients after stent implantation. Magma 1998;6(2–3):184–5.
[23] Lenhart M, Volk M, Manke C, Nitz WR, Strotzer M, Feuerbach S, et al. Stent appearance at contrast-enhanced MR angiography: in vitro examination with 14 stents. Radiology 2000;217(1):173–8.
[24] Bartels LW, Smits HF, Bakker CJ, Viergever MA. MR imaging of vascular stents: effects of susceptibility, flow, and radio-frequency eddy currents. J Vasc Interv Radiol 2001;12(3):365–71.
[25] Camacho CR, Plewes DB, Henkelman RM. Nonsusceptibility artifacts due to metallic objects in MR imaging. J Magn Reson Imaging 1995;5(1):75–88.